

# Voltage Scaling for Partitioned Systolic Array in A Reconfigurable Platform

Rourab Paul<sup>1</sup>, Sreetama Sarkar<sup>2</sup>, Suman Sau<sup>3</sup>, Koushik Chakraborty<sup>4</sup>, Sanghamitra Roy<sup>4</sup> and Amlan Chakrabarti<sup>5</sup>  
 Computer Science & Engineering, Siksha 'O' Anusandhan, Odisha, India<sup>1</sup>  
 Electrical and Computer Engineering Technical University Munich, Germany<sup>2</sup>  
 Computer Science & Information Technology, Siksha 'O' Anusandhan, Odisha, India<sup>3</sup>  
 Dept. Electrical and Computer Engineering, Utah State University, Logan, USA<sup>4</sup>  
 School of IT, University of Calcutta Kolkata, India<sup>5</sup>  
 rourabpaul@soa.ac.in<sup>1</sup>

**Abstract**—The exponential emergence of Field Programmable Gate Array (FPGA) has accelerated the research of hardware implementation of Deep Neural Network (DNN). Among all DNN processors, domain specific architectures, such as, Google’s Tensor Processor Unit (TPU) have outperformed conventional GPUs. However, implementation of TPUs in reconfigurable hardware should emphasize energy savings to serve the green computing requirement. Voltage scaling, a popular approach towards energy savings, can be a bit critical in FPGA as it may cause timing failure if not done in an appropriate way. In this work, we present an ultra low power FPGA implementation of a TPU for edge applications. We divide the systolic-array of a TPU into different FPGA partitions, where each partition uses different near threshold (NTC) biasing voltages to run its FPGA cores. The biasing voltage for each partition is roughly calculated by the proposed offline schemes. However, further calibration of biasing voltage is done by the proposed online scheme. Four clustering algorithms based on the slack value of different design paths study the partitioning of FPGA. To overcome the timing failure caused by NTC, the higher slack paths are placed in lower voltage partitions and lower slack paths are placed in higher voltage partitions. The proposed architecture is simulated in *Artix-7* FPGA using the *Vivado* design suite and Python tool. The simulation results substantiate the implementation of voltage scaled TPU in FPGAs and also justifies its power efficiency.

**Index Terms**—FPGA partition, Low Power, TPU, Voltage Scaling

## I. INTRODUCTION

The configurable logic block (CLB) and switch matrix of FPGAs are power hungry, which makes FPGAs energy inefficient compared to ASICs. Recently many researchers [1], [2] have reported CPU-FPGA based hybrid data center architectures which provides hardware acceleration facility for DNNs. Despite power inefficiency, FPGA becomes popular in the Cloud-Scale acceleration architecture due to its specialized hardware and the economic benefits of homogeneity. Therefore, reducing power in FPGA for DNN applications becomes a very relevant topic of research. Article [3] has studied the timing failure vs biasing voltage of DNN implementation in FPGA. They have underscaled biasing voltage  $V_{ccint}$  of the entire FPGA to increase the power efficiency of Convolution Neural Network (CNN) accelerator by a factor of 3. A single  $V_{ccint}$  for the entire FPGA might not be the most power

efficient solution. Partitioning an FPGA according to the slacks and feeding different biasing voltages for different partitions can cause further reduction of power for CNN implementations. In [4], the authors have implemented a systolic array using near threshold (NTC) biasing voltage in ASIC, which can predict the timing failure of multiplier-accumulators (MACs) placed inside the systolic array of TPU. The prediction of timing failure is based on *Razor* flipflop [5]. Higher fluctuation of input bits increases the possibility of timing failure in NTC condition. In [4], once the timing failure of a MAC is predicted by its internal *Razor* flipflop, the biasing voltage of the MAC is boosted up.

Targeting FPGA based DNN applications [1], our work investigates voltage scaling techniques of TPU in the FPGA platform. Different  $V_{ccint}$  for each of the MACs in a systolic array will be an absurd implementation for FPGA, therefore this work partitions FPGA floor according to the slack value of the path of MACs. Each partition consists a group of paths within the MAC having similar slacks. Each partition is connected with different  $V_{ccint}$ . The proposed methodology abstracts the synthesis timing report from the *Vivado* tool. In a synthesized design, the *Vivado* IDE timing engine estimates the net delays of paths based on connectivity and fanout. The clustering algorithms create some clusters or groups based on path delays. The clusters with higher delays causing lower slack are placed in FPGA partitions with higher  $V_{ccint}$  and the clusters with lower delays causing higher slack are placed in FPGA partitions with lower  $V_{ccint}$ . Here the  $V_{ccint}$  provides power to a FPGA core. The tuning of  $V_{ccint}$  with slack is done by unique *offline – online* strategy. The circuit level challenges on the implementation of voltage scaling in FPGA platform are beyond the present scope of our article. However, the feasibility of implementing the necessary hardware for voltage scaling support is evident considering the successful implementations in other ASIC technologies. As is unavailable in current FPGAs we have simulated the design for the validation of the claim. The contribution of the paper is as follows:

- This paper proposes a new CAD flow to create voltage

scaled TPU in FPGA based platforms considering the trade off of circuit delay against biasing voltage.

- The proposed algorithm divides the systolic array of TPU into different partitions. Each partition will have different  $V_{ccint}$ . The  $V_{ccint}$  in different partitions is scaled against the delay of different slacks.
- The calibration of  $V_{ccint}$  of different partitions is done by the proposed *online* and *offline* scheme.

The organization of the article is as follows: Sec. II outlines our proposed EDA tool flow. Sec. III discusses about the clustering algorithms. The methodology of the proposed work is described in Sec. IV. Result, implementation and conclusion are organized in Sec. V and Sec. VI respectively.

## II. TOOL FLOW

A typical Xilinx FPGA in *Vivado* environment has 3 conventional steps such as synthesis, implementation and bit file generation whereas the adopted tool flow of the proposed partitioned FPGA is divided into two environments: (i) *Vivado* Environment for synthesis, implementation and bit file generation and (ii) Python Environment for clustering similar slacks. The entire tool flow is shown in Fig. 1.

### A. Vivado Environment

The *Vivado* environment is involved with 3 sub-steps stated below:

1) *Synthesis*: *Vivado* synthesis process transforms register transistor logic (RTL) to gate level representation. The synthesis process generates delays of all possible paths of the design. The timing report of the synthesis process contains 12 information such as name of the path, slack value, level, high fanout, path from, path to, total delay of path, logic delay, net delay, time requirement source clock and destination clock as shown in Table I. It is to be noted that the estimation of the slacks of each logic block is at a high level. The actual timing behavior of the design depends on the net delays after placement and routing.

2) *Implementation*: The *Vivado* Implementation process is a timing driven flow that transforms a logical netlist and constraints (Xilinx Design Constraints format) into a placed and routed design to make it ready for the bitstream generation process. In our proposed tool flow, the logical netlist is provided by *Vivado* synthesis process but the Xilinx Design Constraints (XDC) is generated by a python script. The clustered slack values are considered for placing the logic paths in a specific location on the FPGA floor.

3) *Bit File Generation*: Once the placement and routing are completed by the implementation process, the flow generates bitstream of the systolic array. The Xilinx bitstream generation program produces a bitstream for the Xilinx device configuration. If there is any requirement of processor, the design may include software application data.

### B. Python Environment

The contribution of the paper lies in augmenting the standard FPGA design tool flow by incorporating a python-based

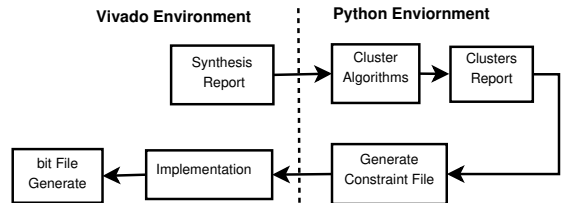


Fig. 1: Tool Flow

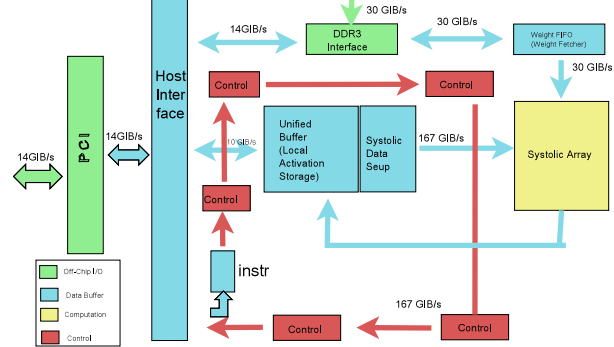


Fig. 2: TPU Architecture

environment, which consists of a script to run three subsequent processes such as choice of *Clustering Algorithms*, *Cluster Generation* and *Constraint Generation*.

1) *Choice of Clustering Algorithms*: A clustering algorithm suited to the requirements is chosen at this step. As stated in Sec. IV, this paper investigates 4 commonly-used clustering algorithms such as Hierarchical, K-means, Mean-shift and DBSCAN.

2) *Cluster Generation*: We have assumed that the FPGA is divided into a few partitions and each partition has a different biasing voltage  $V_{ccint}$ . The clustering algorithms create few groups. The paths having similar slacks form a group and they are placed in the same FPGA partition.

3) *Constraint Generation*: Xilinx uses a constraint file format (XDC) to specify the coordinates of different paths of the proposed systolic array. The XDC file is generated by the python script.

## III. CLUSTERING ALGORITHMS

We have investigated 4 clustering algorithms to group the paths having similar slacks. Algorithms can be chosen based on the design requirements: if we want to set a pre-defined number of clusters, or set hyperparameters to automatically determine the number of clusters. Different algorithms work well for different data distributions. Depending on our design requirements, we choose among the following four algorithms:

### A. Hierarchical

The hierarchical clustering [6] algorithm considers each data point as a single cluster and measures distance between two clusters based on a chosen distance measure (in this case, Euclidean distance). The two clusters that are closest to each other are merged. The process is continued until all clusters have been merged into a single cluster (root of the dendrogram). As shown in fig. 3, the dendrogram is a tree-like structure used for visualizing the hierarchy of clusters. The

TABLE I: A Fragment of Timing Report from Synthesis

Name	Slack	Levels	High Fanout	From	To	Total Delay	Logic Delay	Net Delay	Requirement	Source Clock	Destination Clock
Path 1	5.34	8	8	GEN_REG_I[0].GEN_REG_J[1].uut/prev_activ_reg[1]/C	GEN_REG_I[1].GEN_REG_J[1].uut/sig_mac_out_reg[16]/D	4.37	2.80	1.57	10.00	clk	clk
Path 2	5.49	8	8	GEN_REG_I[0].GEN_REG_J[1].uut/prev_activ_reg[1]/C	GEN_REG_I[1].GEN_REG_J[1].uut/sig_mac_out_reg[15]/D	4.40	2.83	1.57	10.00	clk	clk
Path 3	5.52	9	8	GEN_REG_I[0].GEN_REG_J[1].uut/prev_activ_reg[1]/C	GEN_REG_I[1].GEN_REG_J[1].uut/sig_mac_out_reg[14]/D	4.36	2.89	1.47	10.00	clk	clk
Path 4	5.59	9	8	GEN_REG_I[0].GEN_REG_J[1].uut/prev_activ_reg[1]/C	GEN_REG_I[1].GEN_REG_J[1].uut/sig_mac_out_reg[13]/D	4.30	2.83	1.47	10.00	clk	clk

number of clusters can be decided from the dendrogram. The hierarchical algorithm is computationally expensive for large datasets, having a time complexity of  $O(n^3)$  where  $n$  is the number of data-points. As is evident from the dendrogram, the length of the branch joining the last two clusters is the highest, indicating they are the most dissimilar, followed by the third and fourth clusters. The result of classifying the slack values into 2, 3 and 4 clusters is illustrated in the fig. 4. Different clusters in Figs. 4, 5, 6 and 7 are indicated using different colours.

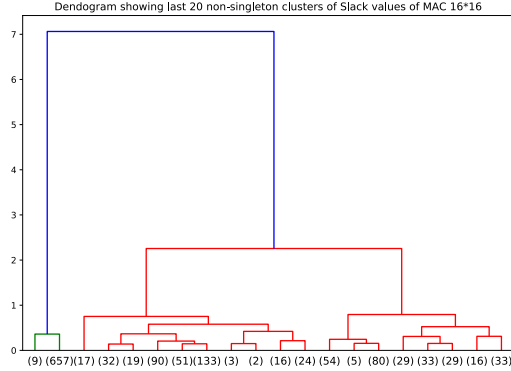


Fig. 3: Dendrogram

### B. K-Means Clustering

K-Means Clustering can cluster data into a predefined number of groups ( $k$ ). At the beginning,  $k$  cluster centers are randomly initialized [7]. The algorithm computes the distance between each data-point and the cluster-centers and assigns data-points to the cluster whose center is closest to it. The cluster centers are then recomputed as the mean of the data-points belonging to that cluster. The process is repeated for a predefined number of steps or until cluster centers do not change significantly. The K-Means Clustering is simple, fast, and its time complexity is  $O(n)$ . Fig. 5 illustrates the results of applying K-Means clustering algorithm on the Slack values of a  $16 \times 16$  Systolic Array for 3, 4 and 5 clusters.

### C. Mean-Shift Clustering

Mean Shift Clustering [8] is based on the idea of Kernel Density Estimation (KDE). KDE assumes that the data points are generated from an underlying distribution and tries to estimate the distribution by assigning a kernel to each data point. The most commonly used kernel is the Gaussian or RBF kernel. The mean-shift algorithm is designed in a way that the points iteratively climb the KDE surface and are shifted to the nearest KDE peaks. It starts with a randomly selected point as the center of the RBF kernel. Thereafter, it proceeds by moving the kernel towards regions of higher density by shifting the center of the kernel to the mean of the points within the window (hence the algorithm is termed mean-shift). This is

continued until shifting the kernel no longer includes more points. This algorithm does not need the number of clusters to be specified beforehand, but it is computationally expensive compared to K-Means (time complexity of  $O(n * \log(n))$  in lower dimension for sklearn implementation). The selection of the window size/radius  $r$  can be non-trivial and plays a key-role in the success of the algorithm. Setting the radius as 0.4 for the slack values of a  $16 \times 16$  Systolic array, yields 4 clusters as observed in the fig. 6.

### D. DBSCAN

The DBSCAN algorithm has two important hyperparameters, based on which it determines the number of clusters [9], **epsilon**: The maximum distance between two samples for one to be considered as in the neighborhood of the other and **minpoints**: The number of samples in a neighborhood for a point to be considered as a core point. At each step, a data-point that has not been visited before is taken. If there are more data-points than *minpoints* within its *epsilon* radius, all the data-points are marked as belonging to a cluster, otherwise the first point is marked as noise. For all points in the newly-formed cluster, points within their ‘*epsilon*’ neighborhood are checked and labeled as either belonging to a cluster or noise. The process is continued until all data-points have been labeled. The greatest advantage of DBSCAN is that it can identify outliers as noise, unlike other algorithms which throw all points into a cluster even if one data point is significantly different from the rest. The time complexity of this algorithm is  $O(n)$  for reasonable *epsilon*. This algorithm is not effective for clusters with varying density since *epsilon* and *minpoints* are different for different clusters.

## IV. OFFLINE-ONLINE SCHEMES

To mitigate timing failure issue in the critical voltage region, we adopted two sequential schemes such as (i) Offline scheme which is involved with FPGA partitioning and rough  $V_{ccinti}$  estimation depending on the FPGA technology. (ii) Online scheme to calibrate suitable  $V_{ccinti}$  for each partition of FPGA using *Razor* flipflop. Each partition of FPGA consists of a group of MACs. All the groups of MACs form systolic array of TPU. Apart from systolic array, TPU has memory to store active and weight inputs, PCI interface, controlling circuitry etc. The architecture of TPU is shown in Fig. 2.

### A. Offline

The proposed offline scheme works on *Vivado* and *Python* environments. As shown in Fig. 1, synthesis is the first step of the proposed tool flow, which takes a netlist of complex logic blocks (CLBs) of systolic array generated from *Vivado* tool. This netlist from the synthesis report is generated after technology mapping and packing stages which contain time slacks of all the possible paths of the systolic array. The

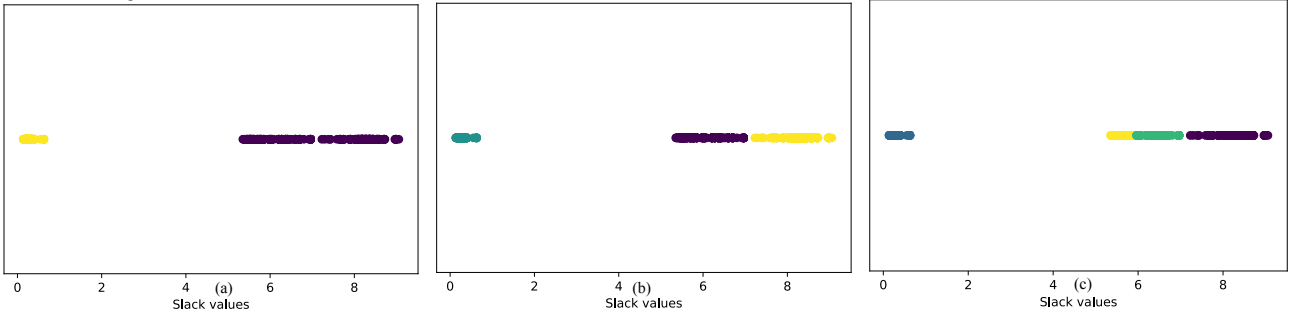


Fig. 4: Hierarchical Cluster of Slack of Systolic Array  $16 \times 16$ : a) #clusters=2, a) #clusters=3, a) #clusters=4

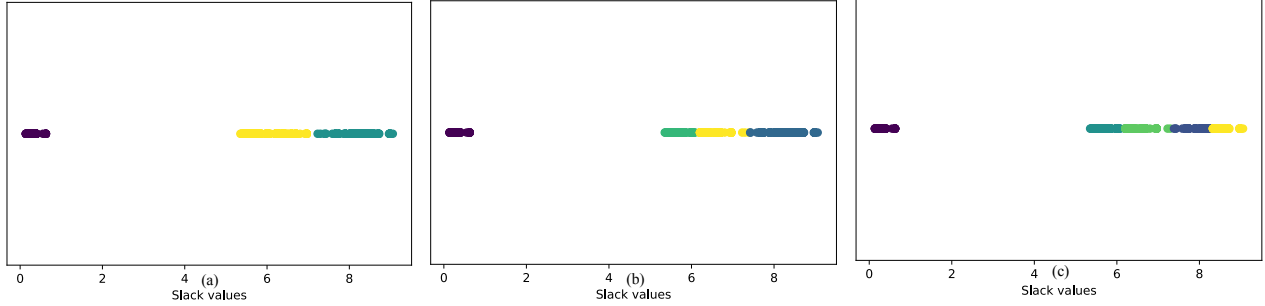


Fig. 5: K Means Cluster of Slack of Systolic Array  $16 \times 16$ : a) #clusters=3, a) #clusters=4, a) #clusters=5

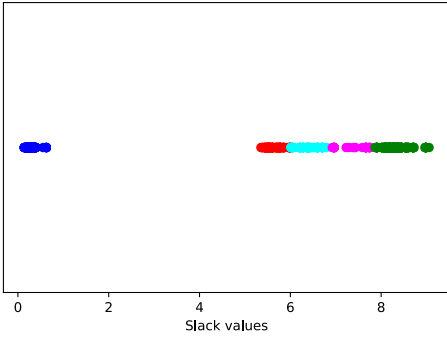


Fig. 6: Mean-Shift Clustering of Slack of Systolic Array  $16 \times 16$

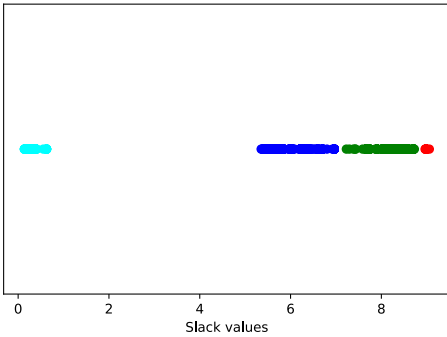


Fig. 7: DB Scan Clustering of Slack of Systolic Array  $16 \times 16$

proposed approach considers only nodes along paths because **(i)** the nodes along the path have data dependencies, which should be placed in the same FPGA partition even without considering the voltage scaling [10]. **(ii)** The slack values of the nodes along paths are usually close to each other. The second step of the proposed methodology is involved with the choice of the clustering algorithm and cluster generation. As stated in Sec. III, the four clustering algorithms such as Hierarchy, K-Mean, Mean-Shift and DBSCAN create multiple

clusters with the paths available in the synthesis report. Even for the same number of clusters, different algorithms classify the data-points slightly differently. The primary concern is to identify clusters of nodes along a path, which can share the slacks available across that path. Even for the same number of clusters, different algorithms classify the data-points slightly differently. Unlike K-means algorithm, the Hierarchical, Mean-Shift and DBSCAN do not need the number of clusters to be specified beforehand. DBSCAN is found to perform the best in this case as it groups together data-points close by, has a reasonable time complexity and can also identify outliers. Hence, clustered paths returned by DBSCAN are chosen for subsequent simulations.

Once the number of clusters is fixed we need to decide the voltage values of different FPGA partitions. In Fig. 8., we illustrate 3 voltage regions in an FPGA, which is also supported by the research work in [3]. The voltage below FPGA crashing voltage  $V_{crash}$  causes timing failure, which reduces the DNN accuracy near to zero. The region between minimum voltage  $V_{min}$  and nominal voltage  $V_{nom}$  is called guardband region where the DNN accuracy will be 100% but power efficiency will be the least. In the critical region, the closer the voltage is to  $V_{crash}$ , higher is the power efficiency and lower the DNN accuracy. Similarly, if  $V_{cint}$  is closer to  $V_{min}$  in the critical region, the power efficiency decreases and DNN accuracy increases. In our proposed architecture, we assume the operating voltage range for the systolic array is  $V_{crash}$  to  $V_{min}$ . If we have  $n$  clusters computed by the chosen clustering algorithm we need  $n$  partitions in FPGA. The primary  $V_{cint}$  estimation for each FPGA partition is computed by Algorithm 1. In Xilinx FPGA, the coordinates of the nets are specified by two parameters  $(X_i, Y_j)$ . Each FPGA partition has range of these coordinates. In the third step of the

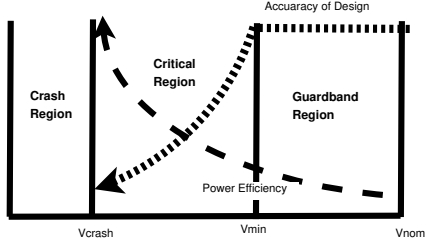


Fig. 8: Voltage behaviour for  $V_{ccint}$

proposed methodology, each clustered path computed by the clustering algorithms is placed in a particular FPGA partition, which is restricted by specific  $X_i, Y_j$  ranges. This restriction is done in the xdc file during *Generate Constraint File* process.

#### Algorithm 1 Voltage Scaling

**Require:**  $V_{ccint}, V_{min}, V_{crash}$  &  $n$

- 1:  $V_b = \frac{V_{min} - V_{crash}}{n}$
- 2: **for**  $i=0$  to  $n-1$  **do**
- 3:    $V_{ccint_i} = \frac{V_l + V_i + V_b}{2}$
- 4:    $V_l = V_l + V_b$
- 5: **end for**

#### B. Online

The  $V_{ccint_i}$  of the  $i^{th}$  FPGA partition calculated by Algorithm 1 is calibrated to  $V_{ccint_i}$  pin of the  $i^{th}$  FPGA partition. The calculation of  $V_{ccint_i}$  by Algorithm 1 is based on the number of partitions  $n$  and the critical voltage region  $V_{min} - V_{crash}$  which solely depends on the type of FPGA technology. However, the appropriate  $V_{ccint_i}$  of the  $i^{th}$  FPGA partition should also depend on the slack values of that partition. At the offline strategy we just calculate a rough estimation of  $V_{ccint_i}$  where as the online strategy calibrates  $V_{ccint_i}$  according to the runtime timing failure of the systolic array. In the online scheme we used one of the most popular online timing error detection scheme, *Razor*, which uses double sampling flipflop to detect timing violation of pipeline stages. The *Razor* flipflop is connected with every MACs of the systolic array to indicate its timing failure. Each MAC has a timing failure flag which is controlled by the *Razor* flipflop. If any timing failure flag of any MAC placed in the  $i^{th}$  FPGA partition is high, the  $V_{ccint_i}$  of that  $i^{th}$  FPGA partition will be increased by one step. If all the timing failure flags of all MACs placed in the  $i^{th}$  FPGA partition is low, the  $V_{ccint_i}$  of that  $i^{th}$  FPGA partition will be decreased by one step. Before starting the actual run of the proposed systolic array, if we have trial run, all the  $V_{ccint_i}$  of all partitions will be tuned accurately by this *online* process. The voltage boosting circuit can be implemented externally following the technique proposed in [11]. In Fig. 9, we have shown that the cluster algorithm partitions the FPGA into 4 islands. The offline scheme as stated in Sec. IV-A calculates 4  $V_{ccint_i}$  such as  $V_{ccint_1}, V_{ccint_2}, V_{ccint_3}$  and  $V_{ccint_4}$  for FPGA partition-1, partition-2, partition-3 and partition-4, respectively. The power distribution unit distributes  $V_{ccint_i}$  such as  $V_{ccint_1}, V_{ccint_2}, V_{ccint_3}$  and  $V_{ccint_4}$  to FPGA partition-1, partition-2, partition-3 and partition-4 respectively.

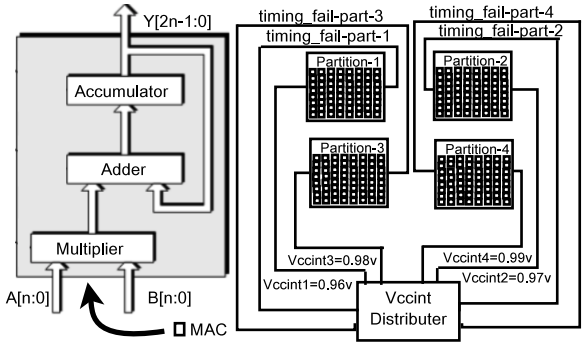


Fig. 9: Example : Partitioned FPGA,  $n=4$

Thereafter, the TPU circuit can be on and the online scheme becomes functional. In Fig. 9, 4 FPGA partitions, partition-1, partition-2, partition-3 and partition-4 have 4 flags from *Razor* flipflops, *timing\_fail - part1*, *timing\_fail - part2*, *timing\_fail - part3* and *timing\_fail - part4* respectively to detect the timing failure of the available partition of the FPGA. The width of the timing failure flag from a specific partition is the number of MACs available in that partition. If any timing failure flag from any FPGA partition becomes high, the  $V_{ccint}$  of that partition will boost up by the power distribution network.

## V. IMPLEMENTATION AND RESULT

As mentioned in Sec. II, the proposed architecture has 2 environments. The clustering algorithms are implemented in Python using the Scikit-learn library. The *synthesis*, *implementation* and *bit file generation* are done by the Vivado using the board support package of Artix-7 FPGA.

#### A. Implementational Challenges

The proposed design could not be implemented as none of the present-day FPGA devices support variable voltage scaling in the different logic partitions. The implementation issues of power distribution unit with multiple  $V_{ccint}$  in different partitions are beyond the scope of our paper. However, we consider, the implementation of voltage scaling technology in ASIC [4] establishes the feasibility of implementation of voltage scaling technology in FPGA.

#### B. Our Validation Strategy

To validate the claim of the proposal, we have partially implemented the proposed scheme. We have designed a  $16 \times 16$  Systolic array, where  $16 \times 16 = 256$  MACs are placed in the FPGA. As an example, one of the clustering algorithm mentioned in Sec. III divides  $16 \times 16$  systolic array into 4 partitions: *partition - 1*, *partition - 2*, *partition - 3* and *partition - 4*. As the current Vivado tool does not allow simulating the design in critical voltage region, our  $16 \times 16$  systolic array is tested in the guardband region. Due to the unavailability of multiple  $V_{ccint}$  support in single a FPGA dice, our design has been implemented in one partition at a time. Therefore, the power measurement of 4 partitions is also done separately where each partition is considered as an individual circuit.

### C. Results

The guardband region for *Artix - 7* FPGA is 0.95 volt to 1.00 volt. For this example  $n = 4$ ,  $V_{min} = V_{nom} = 1.00$  volt,  $V_{crash} = V_{min} = 0.95$  volt, therefor  $V_b = 0.05$  volt. Algorithm 1 calculates the  $V_{ccint_i}$  of the 4 FPGA partitions of this design which are :  $V_{ccint_1} = 0.956$  for *partition-1*,  $V_{ccint_2} = 0.968$  for *partition-2*,  $V_{ccint_3} = 0.985$  for *partition-3* and  $V_{ccint_4} = 0.993$  for *partition-4*. It has been observed that when the partial sums are moved to the bottom rows of systolic array, the timing error increases significantly. Therefore, in this example the MACs of bottom rows may have less slacks, which should be placed in *partition-3* and *partition-4* where  $V_{ccint_i}$  is more compared to the existing  $V_{ccint_i}$ . The MACs of upper rows should have more slacks which should be placed in *partition-1* and *partition-2* where  $V_{ccint_i}$  is less compared to the existing  $V_{ccint_i}$ . As shown in Fig 9, say the clustering algorithm divides the  $16 \times 16$  systolic array into four  $8 \times 8$  systolic array partitions and each partition has  $8 \times 8 = 64$  MACs. We assume the top-left partition-1 consists of a  $8 \times 8$  systolic array which has  $V_{ccint_1} = 0.956 \approx 0.96$ . Similarly, top-right partition-2 has  $V_{ccint_2} = 0.968 \approx 0.97$ , bottom-left partition-3 has  $V_{ccint_3} = 0.985 \approx 0.98$  and bottom right partition-4 has  $V_{ccint_4} = 0.993 \approx 0.99$ . Table II shows the dynamic power consumption for  $V_{ccint_i}$  of 4 partitions which together consumes 382 mW, whereas the systolic array without voltage scaling consumes 408 mW power. Therefore, the adoption of voltage scaling scheme on this  $16 \times 16$  systolic array reduces 6.37% dynamic power consumption for  $V_{ccint_i}$ .

### VI. CONCLUSION

FPGA is becoming popular in DNN based configurable cloud because of its efficiency and manageability but immoderate power consumption is a growing concern for present FPGA technology. A lot of effort has been made to reduce the power consumption by using multiple biasing voltages in FPGA. This paper proposes a TPU architecture where the MACs are placed in different partitions of FPGA based on the slacks of different paths of MACs. Each partition of the FPGA uses different biasing voltage  $V_{ccint}$ . The proposed *online* and *offline* schemes can tune appropriate  $V_{ccint}$  with the group of slacks of MACs which are placed in the partitions. The experimental results show that the voltage scaled systolic array can reduce power consumption. In future we will address two points such as **(i)** Improvement of  $V_{ccint}$  calibration by grouping input sequences with similar delay characteristics to predict future timing failures. **(ii)** Study the tradeoff between the DNN accuracy estimated in terms of timing failures with the no. of partitions and that between no. of partitions and dynamic power. The same partition based voltage scaling can be used for other high performance hardware accelerator to reduce the power consumption.

### REFERENCES

[1] A. M. Caulfield and et. al. A cloud-scale acceleration architecture. In *2016 49th Annual IEEE/ACM International Symposium on Microarchitecture (MICRO)*, pages 1–13, 2016.

TABLE II: Comparison Results

Scheme	Dimension of Systolic Array	Partition No.	$V_{ccint_i}$ volt	Logic Power (mw)	Signal Power (mw)	Clock Power (mw)	Dynamic Power for $V_{ccint}$ (mw)
Without Voltage Scaling	$16 \times 16$	NA	1.00	227	65	115	408
Voltage Scaled	$8 \times 8$	partition-1	0.96	50	15		
	$8 \times 8$	partition-2	0.97	51	16		
	$8 \times 8$	partition-3	0.98	52	16		
	$8 \times 8$	partition-4	0.99	53	16		
<b>% of Reduction</b>				<b>6.37</b>			

[2] A. Putnam and et al. A reconfigurable fabric for accelerating large-scale datacenter services. *IEEE Micro*, 35(3):10–22, 2015.

[3] B. Salami, E. B. Onural, I. E. Yuksel, F. Koc, O. Ergin, A. Cristal Kestelman, O. Unsal, H. Sarbazi-Azad, and O. Mutlu. An experimental study of reduced-voltage operation in modern fpgas for neural network acceleration. In *2020 50th Annual IEEE/IFIP International Conference on Dependable Systems and Networks (DSN)*, pages 138–149, 2020.

[4] P. Pandey, P. Basu, K. Chakraborty, and S. Roy. Greentpu: Improving timing error resilience of a near-threshold tensor processing unit. In *2019 56th ACM/IEEE Design Automation Conference (DAC)*, pages 1–6, 2019.

[5] D. Ernst, Nam Sung Kim, S. Das, S. Pant, R. Rao, Toan Pham, C. Ziesler, D. Blaauw, T. Austin, K. Flautner, and T. Mudge. Razor: a low-power pipeline based on circuit-level timing speculation. In *Proceedings. 36th Annual IEEE/ACM International Symposium on Microarchitecture, 2003. MICRO-36.*, pages 7–18, 2003.

[6] Stanford University. Hierarchical agglomerative clustering. *2008 Cambridge University Press*, 2008.

[7] David Arthur and Sergei Vassilvitskii. K-means++: the advantages of careful seeding. In *In Proceedings of the 18th Annual ACM-SIAM Symposium on Discrete Algorithms*, 2007.

[8] D. Comaniciu and P. Meer. Mean shift: a robust approach toward feature space analysis. *IEEE Transactions on Pattern Analysis and Machine Intelligence*, 24(5):603–619, 2002.

[9] Martin Ester, Hans-Peter Kriegel, Jörg Sander, and Xiaowei Xu. A density-based algorithm for discovering clusters in large spatial databases with noise. In *Proceedings of the Second International Conference on Knowledge Discovery and Data Mining*, KDD’96, page 226–231. AAAI Press, 1996.

[10] R. Mukherjee and Seda Ogrenci Memik. Realizing low power fpgas : A design partitioning algorithm for voltage scaling and a comparative evaluation of voltage scaling techniques for fpgas. 2005.

[11] T. N. Miller, X. Pan, R. Thomas, N. Sedaghati, and R. Teodorescu. Booster: Reactive core acceleration for mitigating the effects of process variation and application imbalance in low-voltage chips. In *IEEE International Symposium on High-Performance Comp Architecture*, pages 1–12, 2012.